the exchange reaction proceeding by the direct attack of the metal ions on the complex (v_a), through intermediates A, B, and C, is

$$v_a = \frac{k_1}{k_{-1}} \frac{k_2 k_3}{k_{-2} + k_3} [\text{Ce(edta)}][M^{2+}] \quad (10)$$

Rate equation (10) can be simplified by taking into account the following considerations. With X = iminodiacetate, we have $k_1/k_{-1} \approx K_{CeX}/K_{CeY} \approx 10^{-9.9}$ and $k_2 \approx K^{-H_2O}{}_M K_{os}$, where K_{os} is the stability constant of the outer-sphere complex formed by the interaction of species A and M^{2+} ($K_{os} \approx 1$). The relative values of k_{-2} and k_3 may be compared by calculating the values $k_{-2} \approx k^{-H_2O}{}_M/K_{MX}$ and $k_3 \approx k^{-H_2O}{}_{Ce}/K_{CeX}$.[11,13] With consideration to these values, rate equation (10) can be written in the following simpler form for the cases of Ni^{2+}, Cu^{2+}, and Co^{2+} as exchanging ion:

$$v_a = k^{-H_2O}{}_M \frac{K_{CeX}}{K_{CeY}} [\text{Ce(edta)}^-][M^{2+}] \quad (11)$$

The significance of the constant b can be established from eq 11. Since this equation gives the exchange rate for the direct attack of the metal ion, the rate constant $k^M{}_{CeY} \approx k^{-M_2O}{}_M K_{CeX}/K_{CeY}$, and thus $b \approx K_{CeX}/K_{CeY}$. This implies that the constant b expresses the probability of the formation of the half-unwrapped intermediates A, which can be approximately given as the ratio of the stability constants of the complexes Ce(imda)$^+$ and Ce(edta)$^-$. When the approximations are taken into account, the agreement between the value $b = 10^{-9.1}$, obtained from the slope in Figure 1, and the ratio $K_{CeX}/K_{CeY} = 10^{-9.9}$ is acceptable.

According to these results the rate of the water loss from the exchanging metal ion plays an important role in the rate-limiting step of the exchange reactions. Similar results were found by Margerum et al. for the exchange reactions of the edta complexes of transition metals.[20]

The protonation of Ce(edta)$^-$ can increase the rate of the formation of the intermediate A. The rate of the exchange proceeding by this pathway is proportional to the concentration of both the M^{2+} and the H^+ ions.

The reaction between Ce(edta)$^-$ and the Pb^{2+} ion proceeds through the formation of the intermediate D. It is known from the results of ^1H NMR studies that the carboxylate–Ln^{3+} ion bonds are labile but that the lifetime of the "free" carboxylate group is very short.[26] As a result of the very high water-exchange rate of the Pb^{2+}(aq) ion the probability of an encounter of a Pb^{2+}(aq) ion that has lost a water molecule with the "free" carboxylate group of Ce(edta)$^-$ in an appropriate position is relatively high, when the binuclear complex D is formed. The rate of transformation of the binuclear complex D into the intermediate B is also low (but probably higher than the rate of formation of B from the intermediate A), and when the concentration of the Pb^{2+} ion is high, the concentration of the binuclear complex D can be significant. Thus the rate-determining step of the reaction here is probably connected with the formation of species B from species D.

Besides the primary importance of water-exchange rates of the attacking metal ion in the exchange reaction, some minor role is played by the concentration ratio of the complex and the metal ion.[9] The exchange reactions can take place in principle through intermediates A, B, and C as well as D, B, and C. If the rate of the water loss of the attacking metal ion is higher than that of the central ion and the concentration of the complex is lower than the concentration of the metal ion, then the exchange takes place predominantly through the intermediates D, B, and C. But when the rate of the water loss of the attacking metal ion is lower and its concentration is not extremely high, then the exchange is slow and predominantly proceeds by the formation of the intermediates A, B, and C.

Registry No. Ce, 7440-45-1; Pb, 7439-92-1; Ni, 7440-02-0; Co, 7440-48-4.

(26) T. H. Sidall and W. E. Stewart, *Inorg. Nucl. Chem. Lett.*, **4**, 421 (1969).

Contribution from the Departments of Chemistry, The Florida State University, Tallahassee, Florida 32306, and University of Houston, Houston, Texas 77004

Solvent and Ligation Effects on the Electroreduction of Chromium Porphyrins[1,2]

LAWRENCE A. BOTTOMLEY and KARL M. KADISH*

Received April 12, 1982

The electroreduction of chloro(5,10,15,20-tetraphenylporphinato)chromium(III) was investigated as a function of solvent, and the identities of all electrode reactants and products were determined via voltammetric and spectroelectrochemical experiments. Detailed oxidation–reduction mechanisms and half-wave potentials are reported for reactions in 10 different nonaqueous solvents. In dichloroethane and DMF both the Cr(II) and Cr(II)-anion-radical species were shown to axially coordinate two substituted pyridine molecules. Formation constants for these adducts were computed from electrochemical titration data. The magnitude of the formation constants was shown to be linearly related to the pK_a of the pyridine nitrogen atom.

Introduction

Despite the recent interest in the chemistry of Cr porphyrins,[3-15] little has been published on the electrochemistry of this system. Ten years ago Fuhrhop, Kadish, and Davis[16,17] reported that (OEP)CrOH could be oxidized in PrCN with single-electron-transfer steps at potentials of 0.79, 0.99, and 1.22 V at a Pt-button electrode. Similarly, single-electron reductions were observed at −1.14 and −1.35 V in Me_2SO. The electron transfers observed at 0.99 and −1.35 V were assigned as the electrogeneration of the π cation and π anion radicals, respectively. These assignments were based in large part on the observed 2.25 ± 0.15 V difference between half-wave potentials for formation of the π anion and π cation radicals with 25 other octaethylporphyrins.[16,17]

*To whom correspondence should be addressed at the University of Houston.

(1) Presented in part at the 157th Meeting of the Electrochemical Society, St. Louis, MO, May 1980 (No. 473), and in part at the 181st Meeting of the American Chemical Society, Atlanta, GA, March 1981 (INOR No. 147).

0020-1669/83/1322-0342$01.50/0

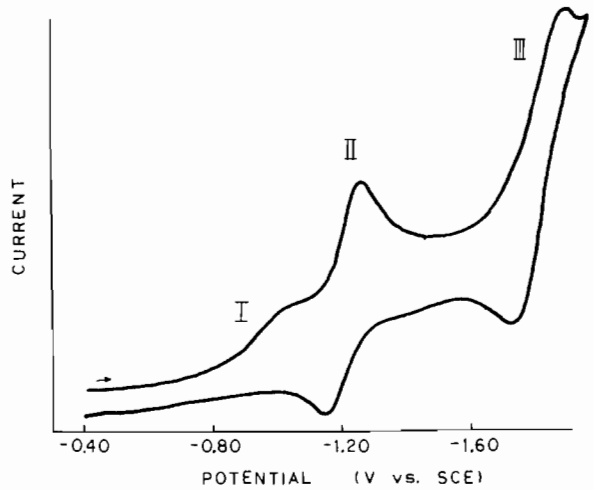

Figure 1. Cyclic voltammogram of (TPP)CrCl dissolved in $EtCl_2$–0.1 M TBAP (scan rate 0.20 V/s): process I, reduction of Cr(III); process II, generation of the π anion radical; process III, generation of the porphyrin dianion.

Newton and Davis[3] later reported that the electrochemical behavior of (TPP)CrCl was unusual and somewhat solvent dependent. They observed two reductions (−1.06 and −1.69 V) and two oxidations (0.87 and 1.25 V) in CH_2Cl_2. In pyridine, new electrode processes were observed after the first potential sweep, indicating the presence of chemical reactions following the electron transfer. However, the electrochemically generated species were not identified in this paper, which concentrated mainly on ESR characterization of metalloporphyrin electrode reactions.

Reed and co-workers[4,7] found three reduction processes for (TPP)CrCl when dissolved in Me_2SO. They assigned the process at −0.86 V to the Cr(III)/Cr(II) couple, the process at −1.23 V to the production of the π anion radical, and the process at −1.70 V to the production of the dianion. These assignments were based on spectral characterization of the reactants and products as well as on the potential difference of 2.25 V between the anion and the cation radical.[16] More recently, Murakami and co-workers[13] published potentials for the three electroreductions observed in DMF (−0.83, −1.09, and −1.72 V) but did not explain the differences between values observed in DMF and those previously reported for other solvents.

In this report, we present a systematic investigation of the effect of solvent on the electrode potentials and mechanism for reduction of (TPP)CrCl in nonaqueous media. Potentials have been measured in 10 different solvents. Electrode products and reactants are identified from the results obtained via voltammetric and spectroelectrochemical experiments. A detailed redox mechanism is presented describing the sequence of reactions that occurs at the electrode in each of the solvents investigated. In addition, formation constants for the addition of substituted pyridine molecules to the Cr(II) and Cr(II)-radical species are reported.

Table I. Peak and Half-Wave Potentials (V) vs. SCE for Reduction of (TPP)CrCl in Selected Solvents

solvent[a]	cyclic voltammetry E_p or $E_{1/2}$	polarography $E_{1/2}$	polarography $E_{3/4} - E_{1/4}$
$EtCl_2$	−1.06[b]	*c*	*c*
CH_2Cl_2	−1.02[b]	*c*	*c*
PhCN	−0.96[b]	−0.92	100
PrCN	−1.00[b]	−0.93	73
$(CH_3)_2CO$	−1.03[b]		
THF	−1.11[b]		
DMF	−0.88	−0.88	63
DMA	−0.91	−0.85	71
Me_2SO	−0.88	−0.89	53
py	see text		

[a] Solvent contains 0.1 M TBAP. Potentials are uncorrected for liquid junctions. [b] Cathodic peak potentials are measured at a scan rate of 100 mV/s. [c] Reduction process overlapped the $(TPP)Cr^{II}$ to anion-radical reactions. See text for details.

Table II. Half-Wave Potentials (V) vs. SCE for the Reversible Formation of the (TPP)Cr Anion Radical in Selected Solvents[a]

solvent	dielec const[b]	DN[b]	$E_{1/2}$	cor $E_{1/2}$[c]
$EtCl_2$	10.36	00.0	−1.18	−1.30
CH_2Cl_2	8.93	00.0	−1.20	−1.28
PhCN	25.2	11.9	−1.18	−1.23
PrCN	20.3	16.6	−1.12	−1.18
$(CH_3)_2CO$	20.70	17.0	−1.10	−1.18
THF	7.58	20.0	−1.21	−1.35
DMF	36.71	26.6	−1.13	−1.21
DMA	37.78	27.8	−1.09	−1.22
Me_2SO	46.68	29.8	−1.25	−1.30
py	12.4	33.1	−1.43	−1.54

[a] Solvent contains 0.1 M TBAP. Potential was measured as $(E_{p,a} + E_{p,c})/2$ on a Pt-button electrode. [b] Sawyer, D. T.; Roberts, J. L., Jr. "Experimental Electrochemistry for Chemists"; Wiley-Interscience: New York, 1974. [c] Potential is corrected for liquid junction by use of the ferrocene/ferrocenium ion approximation.

Experimental Section

Materials. Tetrabutylammonium perchlorate, TBAP (Eastman), was first recrystallized from ethyl acetate and dried in vacuo at 80 °C prior to use. (TPP)CrCl was synthesized as per the method of Summerville et al.[5] The crude product was chromatographed twice on basic alumina (Fisher Scientific). The purity of this material was verified by comparison of the visible spectrum with literature spectra.

Ten different nonaqueous, aprotic solvents were used throughout this study. Me_2SO (Eastman), DMA (Fisher Scientific), and PhCN (Aldrich) were received as reagent grade from the supplier and were dried over 4-Å molecular sieves prior to use. $EtCl_2$ (Mallinckrodt) was purchased as reagent grade. Prior to use, portions were extracted with equal volumes of concentrated H_2SO_4, distilled H_2O, and a 5% KOH solution. The extract was then distilled from P_2O_5 and stored

(2) Abbreviations used: TPP = 5,10,15,20-tetraphenylporphinato dianion; OEP = 2,3,7,8,12,13,17,18-octaethylporphinato dianion; DN = Gutmann donor number; X = monovalent anion; L = ligand molecule; S = solvent molecule; β_n^m = formation constant for the addition of *n* ligand molecules to a metalloporphyrin complex with the metal in the *m* oxidation state; $EtCl_2$ = 1,2-dichloroethane; py = pyridine; PrCN = *n*-butyronitrile; PhCN = benzonitrile; THF = tetrahydrofuran; Me_2SO = dimethyl sulfoxide; DMF = dimethylformamide; DMA = *N,N*-dimethylacetamide; TBAP = tetrabutylammonium perchlorate; (TBA)Cl = tetrabutylammonium chloride.

(3) Newton, C. W.; Davis, D. G. *J. Magn. Reson.* **1975**, *20*, 446–457.
(4) Cheung, S. K.; Grimes, C. J.; Wong, J.; Reed, C. A. *J. Am. Chem. Soc.* **1976**, *98*, 5028–5030.
(5) Summerville, D. A.; Jones, R. D.; Hoffman, B. M.; Basolo, F. *J. Am. Chem. Soc.* **1977**, *99*, 8195–8202.
(6) Basolo, F.; Jones, R. D.; Summerville, D. A. *Acta Chem. Scand., Ser. A* **1978**, *A32*, 771–776.
(7) Reed, C. A.; Kouba, J. K.; Grimes, C. J.; Cheung, S. K. *Inorg. Chem.* **1978**, *17*, 2666–2670.
(8) Scheidt, W. R.; Brinegar, A. C.; Kirner, J. F.; Reed, C. A. *Inorg. Chem.* **1979**, *18*, 3610–3612.
(9) Wayland, B. B.; Olson, L. W.; Siddiqui, Z. U. *J. Am. Chem. Soc.* **1976**, *98*, 94–98.
(10) Groves, J. T.; Kruper, W. J., Jr. *J. Am. Chem. Soc.* **1979**, *101*, 7613–7615.
(11) Groves, J. T.; Kruper, W. J., Jr.; Nemo, T. E.; Myers, R. S. *J. Mol. Catal.* **1980**, *7*, 169–177.
(12) Budge, J. R.; Gatehouse, B. M. K.; Nesbit, M. C.; West, B. O. *J. Chem. Soc., Chem. Commun.* **1981**, 370–371.
(13) Murakami, Y.; Matsuda, Y.; Yamada, S. *J. Chem. Soc., Dalton Trans.* **1981**, 885–861.
(14) Bottomley, L. A.; Kadish, K. M. *J. Chem. Soc., Chem. Commun.* **1981**, 1212–1214.
(15) Buchler, J. W.; Lay, K. L.; Castle, L.; Ullrich, V. *Inorg. Chem.* **1982**, *21*, 842–844.
(16) Kadish, K. M.; Davis, D. G.; Fuhrhop, J. H. *Angew. Chem., Int. Ed. Engl.* **1972**, *84*, 1072–1076.
(17) Fuhrhop, J. H.; Kadish, K. M.; Davis, D. G. *J. Am. Chem. Soc.* **1973**, *95*, 5140–5147.

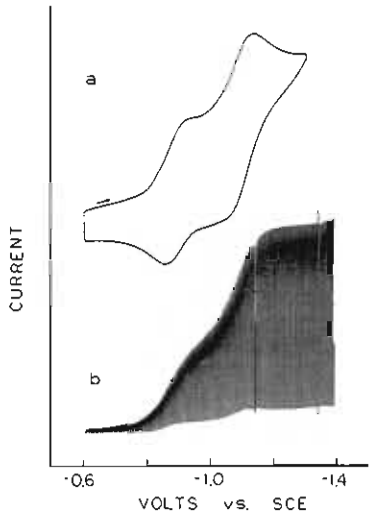

Figure 2. Current–voltage curves for (TPP)CrCl dissolved in DMA–0.1 M TBAP: (a) cyclic voltammogram at a Pt button (scan rate 0.20 V/s); (b) polarogram at a DME.

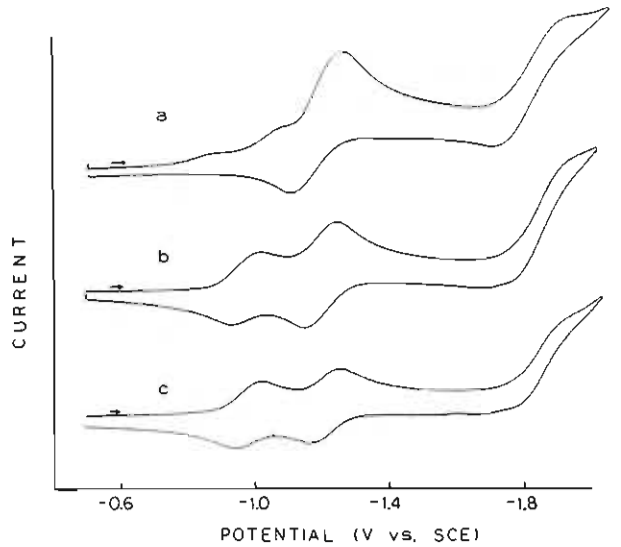

Figure 3. Cyclic voltammograms obtained on a 2.0 mM solution of (TPP)CrCl dissolved in $EtCl_2$–DMF mixtures (scan rate 0.20 V/s). % (v/v) DMF: (a) 0.0; (b) 25; (c) 45.

in the dark over activated 4-Å molecular sieves. CH_2Cl_2, obtained from Fisher Scientific as technical grade, was treated in a similar fashion. PrCN (Aldrich) was purified as per the method of Van Duyne and Reilley.[18] $(CH_3)_2CO$ (MCB) was dried over 4-Å molecular sieves prior to use. THF (MCB) was distilled under N_2 from $LiAlH_4$ just prior to use. DMF was treated with 4-Å molecular sieves after purchase from Baker Chemical Co. When DMF was purchased from Eastman Chemical Co., it was first shaken with KOH, distilled from CaO under N_2, and stored over 4-Å molecular sieves. The substituted pyridines used in this study were obtained from Aldrich Chemical Co. and were purified by standard literature procedures.

Methods. All electrochemical measurements were made with the instrumental equipment previously described.[19] For all electrochemical measurements, the reference electrode was separated from the bulk of solution by means of either a fritted-glass disk or a cracked-glass junction. The solution in the bridge consisted only of solvent and supporting electrolyte. This solution was changed periodically, to prevent aqueous contamination of the cell solution by the reference electrode. Deoxygenation of all solutions was accomplished by passing a constant stream of solvent-saturated, high-purity N_2 through the solution for 10 min and maintaining a blanket of N_2 over the solution while the measurements were made. Half-wave potentials were measured as the average of the anodic and cathodic peak potentials. All potentials are reported vs. the SCE and have a maximum associated uncertainty of ±0.01 V. Electrochemical titrations were performed as previously described.[20]

Visible spectroscopic measurements were made with a Tracor Northern 1710 holographic optical spectrometer/multichannel analyzer. Spectra result from the signal averaging of 100 sequential 5-ms spectral acquisitions.

Results and Discussion

Electron Transfers in CH_2Cl_2 and $EtCl_2$. A cyclic voltammogram typical of the current–voltage curves obtained in either CH_2Cl_2 or $EtCl_2$ is depicted in Figure 1 (for $EtCl_2$). At a Pt electrode, three processes are observed in the potential range −0.60 to −1.90 V. The first process (at 0.10 V/s, $E_{p,c} = -1.06$ V in $EtCl_2$ and −1.02 V in CH_2Cl_2) has a decreased current maximum and a broad shape ($E_p - E_{p/2}$) typical of an irreversible (slow) electron-transfer process. The peak potential was dependent on the scan rate, and there was no observable reoxidation wave, also indicative of a slow electron transfer. The two subsequent processes are quasi-reversible with half-wave potentials at −1.18 and −1.81 V in $EtCl_2$ and at −1.20 and −1.86 V in CH_2Cl_2, respectively. Tables I and II list the potentials for reduction of (TPP)CrCl in each solvent by both cyclic voltammetry and polarography. The first two processes were overlapped when current–voltage curves were obtained at the dropping-mercury electrode (DME) and yielded a composite two-electron transfer. Similar overlapping waves were also obtained when the starting material was (TPP)-$CrClO_4$.[21]

Optical measurements taken after exhaustive electrolysis at −1.30 V in CH_2Cl_2 at an Au minigrid yielded spectra essentially identical with that previously reported for (TPP)-Cr·$2CH_3C_6H_5$.[7] On the basis of these results, the electroreduction pathway for (TPP)CrCl in noncoordinating media is proposed to occur via eq 1 and 2, where the first reaction is

$$(TPP)CrCl \xrightarrow{e^-,\ irrev} (TPP)Cr + Cl^- \qquad (1)$$

$$(TPP)Cr \rightleftharpoons [(TPP)Cr]^- \qquad (2)$$

a rate-controlling slow electron-transfer step. This will be discussed in further detail later in this paper.

Electron Transfers in Weakly Coordinating Media. Current–voltage curves taken of (TPP)CrCl dissolved in weakly coordinating solvents (PrCN, PhCN, $(CH_3)_2CO$, and THF) also are characterized by three electrode processes. At a Pt-button electrode, the first two reduction processes are overlapped, similar to the overlap observed in noncoordinating media. These solvents are classified as weakly coordinating because Summerville et al.[5] have previously shown that (TPP)CrCl exists as a six-coordinate complex about the Cr core, i.e., (TPP)CrCl(S). However, the first and second reduction processes are resolved at the DME. In these solvents, all three processes gave approximately equal maximum currents, indicating that the same number of electrons are involved in each step. Wave analysis on the second process produced slopes of 58 ± 3 mV, indicating an n value of 1. This was confirmed coulometrically. Wave analysis on the first electron transfer in PhCN and PrCN (see Table I) yielded slopes that were greater than that expected for a reversible electrode process. On the basis of these results, reactions 3 and 4 are

(18) Van Duyne, R. P.; Reilley, C. *Anal. Chem.* **1972**, *44*, 142–152.
(19) Bottomley, L. A.; Kadish, K. M. *Inorg. Chem.* **1981**, *20*, 1348–1357.
(20) Kadish, K. M.; Beroiz, D.; Bottomley, L. A. *Inorg. Chem.* **1978**, *17*, 1124–1129.
(21) Kadish, K. M.; Kelly, S.; Bottomley, L. A., unpublished results.

proposed as the electroreduction pathway for (TPP)CrCl in weakly coordinating media.

$$(TPP)CrCl(S) \xrightarrow{e^-,\ irrev} (TPP)Cr + Cl^- + S \quad (3)$$

$$(TPP)Cr \rightleftharpoons [(TPP)Cr]^- \quad (4)$$

Electron Transfers in Coordinating Media—Oxygen Donor Solvents. Figure 2 illustrates the type of cyclic voltammograms obtained for electroreduction of (TPP)CrCl in coordinating solvents with oxygen donor atoms (DMA, DMF, and Me_2SO). In Figure 2 only the first two reduction processes are illustrated. However, in each solvent, three well-resolved, reversible reductions were observed by both cyclic voltammetry and classical polarography. For all processes, peak currents were proportional to the square root of the scan rate. Half-wave potentials for all three processes were invariant with changes in scan rate. The minimum differences in peak potentials for the forward and reverse sweeps were greater than the expected value (59 mV) and ranged from 60 to 90 mV, depending upon the solvent, the process, and the scan rate. The ratios of anodic to cathodic currents for all processes were equal to unity. These data suggest that reductions in oxygen donor media are best described as reversible to quasi-reversible electron transfers.

The striking difference in the current–voltage curves obtained in oxygen donor solvents as compared to those in nonbonding solvents suggests that solvent axial ligation produces reversibility for Cr(III)/Cr(II). Summerville and co-workers[5] have previously shown from conductance data that Cl^- is a nonlabile axial ligand on the Cr center, even in neat Me_2SO. In addition, they have reported spectroscopic evidence that solvents as weakly coordinating as THF and $(CH_3)_2CO$ occupy the sixth coordination site. Interestingly, the current–voltage curves obtained in these solvents are much different from those obtained in DMF, DMA, and Me_2SO. Clearly then, if solvent ligation is responsible for the observed electrochemical differences, changes in Cr(II) coordination seem indicated. Reed and co-workers[7] have previously reported the spectral properties of six-coordinate Cr(II), in (TPP)Cr(L) (where L = nitrogenous base). For a determination of the stoichiometry of Cr(II) that was generated from Cr(III) in our electrode reactions, titrations of each bonding solvent into a (TPP)CrCl–$EtCl_2$ solution were performed. Some of these data are shown in Figure 3 for DMF. As the concentration of DMF increased, no shifts in potential were observed for any process. However, the irreversible, first reduction process ($E_{p,c}$ = −1.06 V at a scan rate of 100 mV/s) decreased in current as a new, reversible process ($E_{1/2}$ = −0.99 V) increased in current. The second, quasi-reversible reduction process (in $EtCl_2$) was transformed into a reversible one as the concentration of DMF increased.

Spectra taken after exhaustive reduction of (TPP)CrCl in DMF ($E_{applied}$ = −1.00 V) yielded absorption maxima at 400, 424, 441 (sh), 566, 605, and 685 nm. Comparison with the published spectra of (TPP)Cr in toluene,[12] and in THF, and the spectrum of $(TPP)Cr(py)_2$ in THF suggests that coordination by DMF (and, by analogy, DMA and Me_2SO) is dissimilar from those of both THF and py. On the basis of these results, eq 5 and 6 are proposed as the electroreduction

$$(TPP)CrCl(S) \rightleftharpoons (TPP)Cr(S) + Cl^- \quad (5)$$

$$(TPP)Cr(S) \rightleftharpoons [(TPP)Cr]^- + S \quad (6)$$

pathway for (TPP)CrCl in oxygen donor media. Although we cannot rule out the possibility of diadduct formation to Cr(II) by oxygen donor solvents, the assignment of a monoadduct is preferred on the basis of preliminary competitive equilibrium studies between DMF and py.[21]

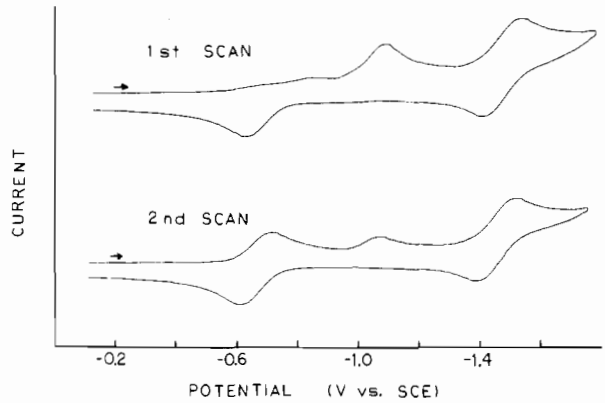

Figure 4. Cyclic voltammogram of (TPP)CrCl dissolved in pyridine (scan rate 0.20 V/s).

Scheme I

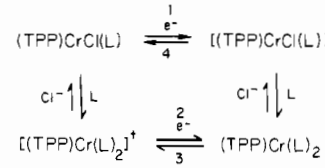

Electron Transfers in Coordinating Media—Nitrogen Donor Solvents. We have previously shown[14] that, in Et_2Cl_2 containing 1.0 M nitrogen donor bases, the current–voltage curves suggest two discrete pathways for electroreduction of (TPP)CrCl as shown in Scheme I.

The reversibility of electron-transfer processes 1 and 4 and the presence of four distinct Cr species at the electrode surface were confirmed by results of cyclic differential-pulse voltammetry (CDPV). Scanning from −0.3 to −1.2 V and then back to −0.3 V, we observed two reduction peaks (1 and 2) and two oxidation peaks (3 and 4) with CDPV. On the cyclic voltammetric time scale, process 4 was not observed, indicating that the symmetrically substituted Cr(II) species is thermodynamically favored over the asymmetrically substituted species $[(TPP)CrCl(L)]^-$. However, at slow scan rates, a measurable amount of $[(TPP)CrCl(L)]^-$ was oxidized (process 4). This species is not present in the bulk of the solution but is produced by the slow reassociation of Cl^- before electron transfer. The driving force behind this reassociation is the relative ease with which $[(TPP)CrCl(L)]^-$ can be oxidized with respect to $(TPP)Cr(L)_2$, that is, the 300-mV difference in oxidation potentials between the two complexes. In the same manner, $[(TPP)Cr(L)_2]^+$ was not present initially in the bulk of solution but was formed at the electrode surface by dissociation of (TPP)CrCl(L) prior to electron transfer.[14] Without the application of a potential this species would not be observed.

Figure 4 depicts cyclic voltammograms obtained on (TPP)CrCl dissolved in py. On the first potential scan from 0.0 to −1.8 V, two single-electron-transfer processes are observed corresponding to the formation of a Cr(II) and a Cr(II)-radical species. The initial reduction process at $E_{p,c}$ = −1.03 V (measured at scan rate of 0.20 V/s) has no coupled oxidation process on the time scale of the experiment, whereas the formation of the Cr(II) radical occurs reversibly ($E_{1/2}$ = −1.43 V). If a second potential scan is initiated immediately after cessation of the first, two separate processes are observed ($E_{p,c}$ = −0.73 and −1.03 V) for electroreduction of (TPP)CrCl. On the second and all subsequent scans, the reduction process at $E_{p,c}$ = −0.73 V has increased in current in proportion to the decrease in current measured for the process at $E_{p,c}$ = −1.03 V. Also, the process at $E_{p,c}$ = −0.73 V is coupled to the process at $E_{p,a}$ = −0.61 V. From peak shapes and the dependence of

Table III. Half-Wave Potentials[a] (V) for the Electroreduction of (TPP)CrCl in $EtCl_2$, Which Was 1.0 M in the Selected Substituted Pyridine

py substituent	pK_a[b]	$E_{1/2}$ for $[(TPP)Cr(L)_2]^+/(TPP)Cr(L)_2$	E_p[c] for (TPP)CrCl(L)/ $(TPP)Cr(L)_2$	$E_{1/2}$ for $(TPP)Cr(L)_2/[(TPP)Cr(L)_2]^-$
3,5-Cl_2	0.67	−0.54	−0.90	−1.33
3-CN	1.40	−0.61	−0.90	−1.31
4-CN	1.86	−0.59	−0.92	
3-Cl	2.81	−0.68	−0.91	−1.39
3-Br	2.84	−0.68	−0.91	−1.41
3-$COCH_3$	3.18	−0.69	−0.93	−1.40
4-$COCH_3$	3.51	−0.69		
H	5.23	−0.76	−0.99	−1.49
3-CH_3	5.79	−0.77	−0.98	−1.49
4-CH_3	5.98	−0.76	−1.00	−1.50
3,4-$(CH_3)_2$	6.46	−0.79	−1.00	−1.52

[a] Potentials are uncorrected for liquid junction and are referenced to the SCE. [b] Values are taken from: Schoefield, K. "Hetero-Aromatic Nitrogen Compounds"; Plenum Press: New York, NY, 1967; p 146. [c] E_p was measured by differential-pulse voltammetry.

both peak currents and peak potentials on scan rate, the presence of chemical reactions coupled to reversible electron transfers is indicated.

Standard thin-layer spectroelectrochemical methodologies were employed in an attempt to characterize the reactants and products of each process. At an applied potential of 0.00 V, the spectrum observed corresponded to that obtained for (TPP)CrCl(py). After complete reduction at −1.2 V, the spectrum was comparable to that reported[7] for $(TPP)Cr(L)_2$, the bisadduct of Cr(II). Finally, the spectrum taken after complete reoxidation at ≃−0.3 V was a mixture of peaks and decayed over the course of several seconds to the spectrum of the starting material, (TPP)CrCl(py). On the basis of these results, electrode reactions 7a and 7b are proposed for the

$$(TPP)CrCl(py) \xrightarrow[E_{p,c} = -1.03\ V]{e^-} [(TPP)CrCl(py)]^- \quad \text{first scan} \quad (7a)$$

$$[(TPP)Cr(py)_2]^+ \xrightarrow[E_{p,c} = -0.73\ V]{e^-} (TPP)Cr(py)_2 \quad \text{second scan} \quad (7b)$$

initial reduction processes in py. Electroreduction of the unsymmetrically substituted, six-coordinate Cr(III) porphyrin, (TPP)CrCl(py), proceeds through the intermediate $[(TPP)CrCl(py)]^-$ to the symmetrically substituted Cr(II) species, $(TPP)Cr(py)_2$. Oxidation of this species at $E_{p,a} = -0.61$ V (Figure 4) produces a symmetrically substituted, six-coordinate Cr(III) species, $[(TPP)Cr(py)_2]^+$. This latter species is subject to a ligand-exchange reaction with free Cl^- to form the original (TPP)CrCl(py) complex, which is also reduced on the second scan as seen in Figure 4. This mechanism is similar to that previously published[14] for electroreduction of (TPP)CrCl in $EtCl_2$-substituted pyridine mixtures. In the latter case, oxidation of the Cr(II) species, $(TPP)Cr(L)_2$, was observed to proceed by either of two pathways, i.e., by direct electron transfer to form the symmetrically substituted Cr(III) species, $[(TPP)Cr(L)_2]^+$, or by ligand exchange to form the Cr(II) species, $[(TPP)CrCl(L)]^-$, followed by oxidation to the starting material, (TPP)CrCl(L). In neat py, there is no evidence for oxidation of $[(TPP)CrCl(py)]^-$ at the electrode. This is presumably due to an extremely short lifetime of the $[(TPP)CrCl(py)]^-$ species in neat solvent.

For a determination of whether or not the Cr(II)-radical species axially coordinated any solvent molecules, electrochemical titrations were performed. Current–voltage curves of (TPP)CrCl dissolved in various $EtCl_2$–py mixtures were taken in a potential range from −1.00 to −1.60 V. The shift in peak potentials over the bulk pyridine concentration range $10^{-3} < C_{py} < 10^{-2}$ M indicates that the Cr(II) species is reduced by the pathway

$$(TPP)Cr(py)_2 \overset{e^-}{\rightleftharpoons} [(TPP)Cr]^- + 2py \quad (8)$$

Over the range $10^{-2} < C_{py} < 0.4$ M, peak potential shifts with increasing [py], indicating that the reaction sequence (9)–(11)

$$(TPP)Cr(py)_2 \xrightarrow{e^-} [(TPP)Cr(py)_2]^- \quad (9)$$

$$[(TPP)Cr(py)_2]^- \xrightarrow{k_f} [(TPP)Cr]^- + 2py \quad (10)$$

$$[(TPP)Cr]^- + 2py \xrightarrow{-e^-} (TPP)Cr(py)_2 \quad (11)$$

occurs at the electrode. Over the range of $0.40 < C_{py} < 2.00$ M, peak potentials were invariant with changes in [py]. Anodic and cathodic peak currents were equal in magnitude and were proportional to the square root of the scan rate. $|E_{p,a} - E_{p,c}|$ values varied between 57 and 62 mV at potential scan rates equal to or less than 0.50 V/s. These results indicate that at high [py] ($C_{py} > 0.40$ M) the generation of the Cr(II) radical proceeds (as in reaction 12) without any change in the number of axial ligands.

$$(TPP)Cr(py)_2 \rightleftharpoons [(TPP)Cr(py)_2]^- \quad (12)$$

Ligand Addition to $(TPP)Cr^{II}$. Basolo and co-workers[5,6] published the first systematic investigation of axial ligation to Cr(III) metalloporphyrins in nonaqueous media. From the results of spectroscopic and conductometric experiments, they demonstrated that (TPP)CrCl will readily coordinate Lewis bases containing oxygen, sulfur, or nitrogen donor atoms to form the unsymmetrically substituted, six-coordinate Cr(III) species, (TPP)CrCl(L). They observed that nitrogenous bases readily displaced molecules with either oxygen or sulfur donor atoms from the Cr(III) center, but not Cl^-. Formation constants for addition of selected nitrogenous bases measured for Cr(III) ranged from 1.26×10^2 to 5.13×10^6 M^{-1}.

In this study incremental additions of py into a solution of (TPP)CrCl dissolved in $EtCl_2$ resulted in the shift in potentials described above (see reactions 8–12 and the adjoining text) and previously.[14] Similar results were obtained for 11 differently substituted pyridines. Table III lists the half-wave potentials for the two reversible processes and the peak potential for the one irreversible process, which was observed in the presence of each substituted pyridine. This latter potential, E_p, was determined by differential-pulse voltammetry.

It is interesting to note that the reduction potential for each process becomes increasingly negative as the pK_a of the pyridine nitrogen donor atom increases. This indicates that axial ligation of the Cr center results in a preferential stabilization of the Cr(III) oxidation state over that for Cr(II) and at the same time of the Cr(II) oxidation state over that for the Cr(II) anion radical. Basolo and co-workers[5,6] reported log (formation constants) ranging from 2.10 to 6.70 for addition of one nitrogenous base molecule to the Cr(III) species on the basis of spectroscopic measurements. We were unable to compute formation constants for ligand addition to Cr(III) from our electrochemical data in $EtCl_2$ because the Cr(III) to Cr(II) reduction in neat $EtCl_2$ is an irreversible one. The Cr(III) to Cr(II) redox process is an irreversible one in all noncoordinating or weakly coordinating solvents. Reversible reactions occur in coordinating solvents (with the exception of pyridine, as noted in the section on solvent effects). Ligand-addition studies in these solvents must then take into account the effect of displacement of solvent molecules from the axial positions on the Cr center. In this study we have selected DMF as a solvent for investigating these solvent displacement reactions

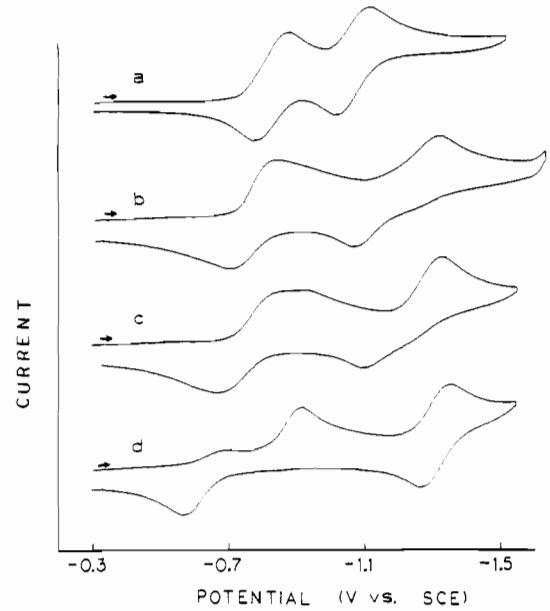

Figure 5. Cyclic voltammograms obtained during the titration of a 2.0 mM solution of (TPP)CrCl dissolved in DMF with pyridine (scan rate 0.20 V/s). Bulk concentration of pyridine: (a) 0.0 mM; (b) 7.3 mM; (c) 36.0 mM; (d) 610 mM.

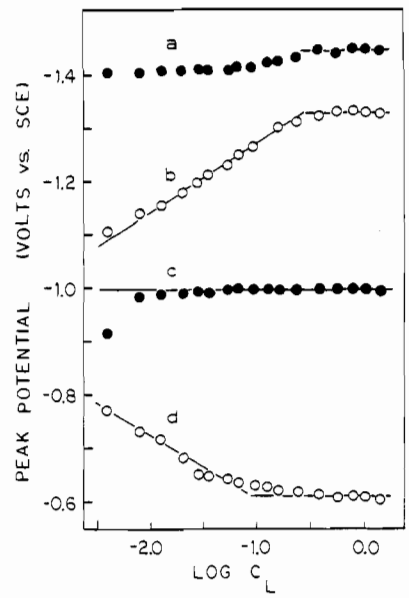

Figure 6. Plot of peak potential vs. the bulk 4-picoline concentration as measured during the titration of a 2.0 mM solution of (TPP)CrCl dissolved in DMF: (a) $E_{p,c}$ for the Cr(II) to Cr(II)-radical reduction; (b) $E_{p,a}$ for the Cr(II)-radical oxidation; (c) $E_{p,c}$ for the Cr(III) to Cr(II) reduction; (d) $E_{p,a}$ for the Cr(II) oxidation. Potentials were measured at a Pt button at a scan rate of 0.20 V/s.

since the redox processes are reversible and DMF acts as a rather weak ligand.

Additions of aliquots of each substituted pyridine into a solution of (TPP)CrCl dissolved in DMF resulted in a substantial change in redox mechanism. This is shown in Figure 5, which depicts four cyclic voltammograms taken as the bulk pyridine concentration was increased from zero to 1.0 M.

Over the ligand concentration range from 1.0 to 40 mM, two forms of Cr(III) were present in equilibrium and the Cr(III) to Cr(II) reduction occurred in two discrete processes. Addition of small amounts of py to solutions resulted in an anodic displacement of the Cr(III) to Cr(II) reduction process ($E_{p,c}$ shifted from −0.88 to −0.81 V) and a cathodic displacement of the Cr(II) to Cr(II)-radical reduction process ($E_{p,c}$ shifted from −1.11 to −1.31 V). The process at $E_{p,c}$ = −0.81 V increased in current with a proportionate decrease in the current associated with the process at $E_{p,c}$ = −0.88 V. The formation of the peak at $E_{p,c}$ = −1.31 V was complete after the addition of only 3 equiv of py into solution. These data suggest that the Cr(II) species has a strong affinity for py. The affinity of (TPP)CrCl for py is also suggested by the transformation of the cyclic voltammograms between parts b and d in Figure 5.

Table IV. Half-Wave Potentials[a] (V) for the Electroreduction of (TPP)CrCl in DMF, Which Was 1.0 M in the Selected Substituted Pyridine

py substituent	p*Ka*[b]	$E_{1/2}$ for $[(TPP)Cr(L)_2]^+/(TPP)Cr(L)_2$	$E_{p,c}$ for $(TPP)CrCl(L)/(TPP)Cr(L)_2$[c]	$E_{1/2}$ for $(TPP)Cr(L)_2/[(TPP)Cr(L)_2]^-$
3,5-Cl_2	0.67		−0.76	−1.14
3-CN	1.40		−0.76	−1.17
4-CN	1.86	−0.63	−0.84	−1.11
3-Cl	2.81	−0.64	−0.86	−1.22
3-Br	2.84	−0.63	−0.90	−1.25
3-$COCH_3$	3.18	−0.63	−0.92	−1.27
4-$COCH_3$	3.51	−0.60	−0.93	
H	5.23	−0.64	−0.91	−1.34
3-CH_3	5.79	−0.64	−0.95	−1.35
4-CH_3	5.98	−0.65	−0.96	−1.36
3,4-$(CH_3)_2$	6.46	−0.66	−1.02	−1.39

[a] Potentials are uncorrected for liquid junction and are referenced to the SCE. [b] Values are taken from: Schoefield, K. "Hetero-Aromatic Nitrogen Compounds"; Plenum Press: New York, NY, 1967; p 146. [c] $E_{p,c}$ was measured at a scan rate of 0.20 V/s.

A third Cr(III) to Cr(II) reduction process is observed at [py] > 7.3 mM. When the pyridine concentration was increased, the reduction process at $E_{p,c}$ = −0.81 V decreased in current with a concomitant formation of a new reduction process at $E_{p,c}$ = −0.91 V. This preferential stabilization of the Cr(III) species over the Cr(II) adduct can only be explained by complexation of (TPP)CrCl with py. Analysis of both peak current and peak potential dependences on scan rate for all reduction processes indicated that the Cr(III) to Cr(II) and the Cr(II) to Cr(II)-radical reductions were coupled to fast chemical reactions following the electron transfer at all concentrations of py.

As seen in Figure 5, the anodic peak potential associated with the Cr(II)-radical to Cr(II) oxidation process also shifts cathodically with increasing py concentration ($E_{p,a}$ shifts from −1.01 to −1.27 V) whereas the Cr(II) to Cr(III) oxidation process shifts anodically with increasing py concentration ($E_{p,a}$ shifts from −0.77 to −0.57 V). These data further confirm the strong affinity Cr(II) porphyrin has for forming axial adducts. Similar results were obtained for all 11 substituted pyridines used.

So that the identity of all species at the electrode could be ascertained, the peak potentials for each process were plotted against the bulk concentration of ligand. Figure 6 depicts the peak potential–log C_L relationships obtained with 4-picoline as the titrant and is representative of the plots obtained for all 11 substituted pyridines. Traces a and c represent the peak potentials observed for 4-picoline as the potential is swept cathodically from −0.40 V whereas traces b and d represent the peak potentials observed on the anodic potential sweep starting from −1.50 V. Above 10 equiv of ligand, $E_{p,c}$ values for both reduction processes are essentially invariant with increasing ligand concentration. Over the ligand concentration range 1 mM < [L] < ~0.70 M (depending upon the ligand used) $E_{p,a}$ for oxidation of the Cr(II) radical to Cr(II) shifted cathodically by 120 mV/10-fold increase in ligand concentration, indicating that Cr(II) was forming a diadduct. This assignment was confirmed by the shift in oxidation peaks for Cr(II)/Cr(III). For this process, peak potentials (trace d)

Scheme II

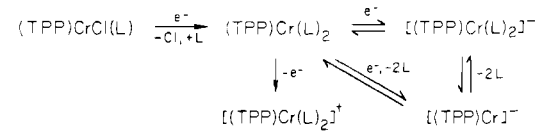

Table V. Formation Constants[a] for Addition of Two Molecules of Selected Substituted Pyridines to (TPP)Cr^{II} and $[(TPP)Cr^{II}]^-$ in DMF

py substituent	pK_a[b]	$\log \beta_2{}^{II}$	$\log \beta_2{}^{R}$
3,5-Cl_2	0.67	2.5	1.6
3-CN	1.40	3.2	2.2
4-CN	1.86	4.4	
3-Cl	2.81	3.8	1.3
3-Br	2.84	4.5	2.0
3-$COCH_3$	3.18	4.9	1.8
4-$COCH_3$	3.51	4.2	
H	5.23	5.0	1.0
3-CH_3	5.79	5.4	1.4
4-CH_3	5.98	5.9	1.1
3,4-$(CH_3)_2$	6.46	6.1	0.9

[a] Formation constants were computed from potential shift data and have a maximum estimated uncertainty of ±0.18 in the log β value. [b] Values are taken from: Schoefield, K. "Hetero-Aromatic Nitrogen Compounds"; Plenum Press: New York, NY, 1967; p 146.

shifted anodically by 119 mV/10-fold increase in ligand concentration. These results are best represented by the following electron-transfer reaction for Cr(II) at low ligand concentration:

$$(TPP)Cr(L)_2 \overset{e^-}{\rightleftharpoons} [(TPP)Cr]^- + 2L \qquad (13)$$

At higher ligand concentrations (above 0.70 M for 4-picoline) potentials for all electron transfers were invariant with changes in ligand concentration. This indicated that all species in the electrode reaction were complexed by an equal number of ligands.

The peak potentials $E_{p,c}$ and $E_{p,a}$ for the Cr(II)/Cr(II)-radical couple were separated by ~80 mV and were characterized as being chemically reversible but electrochemically quasi-reversible by conventional cyclic voltammetric analysis. The Cr(III)/Cr(II) couple, however, was separated by 130–250 mV, depending upon the identity of the ligand. Table IV lists the potentials obtained for each electron-transfer process and for each ligand. Conventional scan rate analysis confirmed that the two peaks for Cr(III)/Cr(II) were chemically coupled. Combination of these results with those observed at low ligand concentration yields the overall mechanism for reduction of (TPP)CrCl(L) shown in Scheme II. Interestingly, the potential for reduction of the unsymmetrically substituted Cr(III) species, (TPP)CrCl(L), shifts cathodically with increasing pK_a of the ligand (see Table IV) whereas potentials for reduction of the symmetrically substituted Cr(III) species, $[(TPP)Cr(L)_2]^+$, are essentially invariant with ligand pK_a. This contrasts with the trend observed in $EtCl_2$–substituted pyridine mixtures (Table III). No explanation for this behavior is evident at this time.

From the potential dependences on ligand concentration, formation constants for addition of two molecules of the substituted pyridine to (TPP)Cr^{II} and $[(TPP)Cr^{II}]^-$ were computed and are listed in Table V. As seen in this table, complexation of (TPP)Cr^{II} by substituted pyridines becomes more thermodynamically favored with increasing ligand pK_a. However, the opposite is true for complexation of the anion radical $[(TPP)Cr^{II}(L)_2]^-$. Plots of log β_2 for each species vs. ligand pK_a were constructed and are depicted in Figure 7. Interestingly, both yield linear traces, but with opposite slopes,

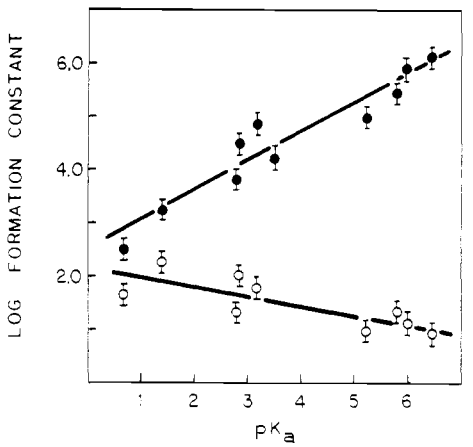

Figure 7. Plots of the log of the formation constant for addition of two molecules of various substituted pyridines vs. the pK_a of the pyridine nitrogen atom for the reactions (TPP)Cr(DMF) + 2L ⇌ (TPP)$Cr(L)_2$ + DMF (closed circles) and $[(TPP)Cr]^-$ + 2L ⇌ $[(TPP)Cr(L)_2]^-$ (open circles).

which are described by eq 14 and 15, respectively. The positive

$$\log \beta_2{}^{II} \text{ (for } (TPP)Cr(L)_2) = 0.55pK_a + 2.46 \qquad (14)$$

$$\log \beta_2{}^{R} \text{ (for } [(TPP)Cr(L)_2]^-) = -0.16pK_a + 2.10 \qquad (15)$$

slope for the log $\beta_2{}^{II}$ vs. pK_a plot for Cr(II) is consistent with σ bonding being the predominant mode of ligand to metal interaction. The magnitude of the slope compares with slopes of 0.24–0.46 obtained from similar plots of log β_1 vs. pK_a for formation of other (TPP)M(L) complexes (where M = Zn(II),[22] Mg(II),[23] Cd(II),[24] Hg(II),[24] Mn(II),[25] and Fe(II)[26]) with the same series of ligands. The slope of 0.55 is also somewhat larger than the value of 0.38 obtained by Basolo and co-workers[5] for complexation of (TPP)Cr^{II} by pyridines in acetone. It is interesting to note the negative slope for the complexation of the Cr(II)-radical species. In contrast, coordination of $[(TPP)Zn]^-$ by one substituted pyridine yielded a $\Delta \log \beta/\Delta pK_a$ value of 1.31.[22] The negative $\Delta \log \beta_2{}^{R}/\Delta pK_a$ value observed for Cr may manifest the increased Coulombic repulsion between the lone pair of electrons on the ligand and the negative charge of the porphyrin π anion radical. Diadduct formation implies an in-plane Cr(II) center and pulls the ligand lone pair toward the porphyrin ring. Coulombic repulsion may not have been operative in the case of the Zn π anion radical because the monoadduct formed has the Zn center displaced from the porphyrin plane toward the ligand. Complexation studies of other π anion metalloporphyrins with the ligand series used herein are under way and will test this postulate.

Acknowledgment. The authors gratefully acknowledge support of this research from the National Science Foundation (Grant CHE-7921536). We also wish to thank Dr. R. K. Rhodes for assistance with the spectral measurements. L.A.B. acknowledges financial assistance from a Florida State COFRS grant.

Registry No. (TPP)CrCl, 28110-70-5; $[(TPP)Cr^{II}]^-$, 83681-22-5; $[(TPP)Cr(3,5\text{-}Cl_2\text{-}py)_2]^+$, 83664-99-7; $[(TPP)Cr(3\text{-}CN\text{-}py)_2]^+$, 83665-00-3; $[(TPP)Cr(4\text{-}CN\text{-}py)_2]^+$, 83665-01-4; $[(TPP)Cr(3\text{-}Cl\text{-}py)_2]^+$, 83665-02-5; $[(TPP)Cr(3\text{-}Br\text{-}py)_2]^+$, 83665-03-6; $[(TPP)Cr(3\text{-}COCH_3\text{-}py)_2]^+$, 83665-04-7; $[(TPP)Cr(4\text{-}COCH_3\text{-}py)_2]^+$,

(22) Kadish, K. M.; Shiue, L. R.; Rhodes, R. K.; Bottomley, L. A. *Inorg. Chem.* **1981**, *20*, 1274–1277.
(23) Kadish, K. M.; Shiue, L. R. *Inorg. Chem.* **1982**, *21*, 1112–1115.
(24) Kadish, K. M.; Shiue, L. R. *Inorg. Chem.* **1982**, *21*, 3623.
(25) Kadish, K. M.; Kelley, S. L. *Inorg. Chem.* **1979**, *18*, 2168–2971.
(26) Bottomley, L. A.; Olson, L.; Kadish, K. M. In "Electrochemical and Spectroscopic Studies on Biological Redox Components"; Kadish, K. M., Ed.; American Chemical Society: Washington, DC, 1982; Adv. Chem. Ser. No. 201, p 279.

83665-05-8; $[(TPP)Cr(py)_2]^+$, 83665-06-9; $[(TPP)Cr(3\text{-}CH_3\text{-}py)_2]^+$, 83665-07-0; $[(TPP)Cr(4\text{-}CH_3\text{-}py)_2]^+$, 83665-08-1; $[(TPP)Cr(3,4\text{-}(CH_3)_2\text{-}py)_2]^+$, 83665-09-2; $(TPP)Cr(3,5\text{-}Cl_2\text{-}py)_2$, 83665-10-5; $(TPP)Cr(3\text{-}CN\text{-}py)_2$, 83665-11-6; $(TPP)Cr(4\text{-}CN\text{-}py)_2$, 83665-12-7; $(TPP)Cr(3\text{-}Cl\text{-}py)_2$, 83665-13-8; $(TPP)Cr(3\text{-}Cr\text{-}py)_2$, 83665-14-9; $(TPP)Cr(3\text{-}COCH_3\text{-}py)_3$, 83665-15-0; $(TPP)Cr(4\text{-}COCH_3\text{-}py)_2$, 83665-16-1; $(TPP)Cr(py)_2$, 67113-84-2; $(TPP)Cr(3\text{-}CH_3\text{-}py)_2$, 67113-85-3; $(TPP)Cr(4\text{-}CH_3\text{-}py)_3$, 67113-86-4; $(TPP)Cr(3,4\text{-}(CH_3)_2\text{-}py)_2$, 83665-17-2; $(TPP)CrCl(3,5\text{-}Cl_2\text{-}py)$, 81329-11-5; $(TPP)CrCl(3\text{-}CN\text{-}py)$, 81329-12-6; $(TPP)CrCl(4\text{-}CN\text{-}py)$, 65013-14-1; $(TPP)CrCl(3\text{-}Cl\text{-}py)$, 81329-13-7; $(TPP)CrCl(3\text{-}Br\text{-}py)$, 81329-14-8; $(TPP)CrCl(3\text{-}COCH_3\text{-}py)$, 81329-15-9; $(TPP)CrCl(py)$, 65013-13-0; $(TPP)CrCl(3\text{-}CH_3\text{-}py)$, 81329-17-1; $(TPP)CrCl(4\text{-}CH_3\text{-}py)$, 81329-18-2; $(TPP)CrCl(3,4\text{-}(CH_3)_2\text{-}py)$, 65013-15-2; $[(TPP)Cr(3,5\text{-}Cl_2\text{-}py)_2]^-$, 83665-19-4; $[(TPP)Cr(3\text{-}CN\text{-}py)_2]^-$, 83665-20-7; $[(TPP)Cr(3\text{-}Cl\text{-}py)_2]^-$, 83665-21-8; $[(TPP)Cr(3\text{-}Cr\text{-}py)_2]^-$, 83665-22-9; $[(TPP)Cr(3\text{-}COCH_3\text{-}py)_2]^-$, 83665-23-0; $[(TPP)Cr(py)_2]^-$, 83665-24-1; $[(TPP)Cr(3\text{-}CH_3\text{-}py)_2]^-$, 83665-25-2; $[(TPP)Cr(4\text{-}CH_3\text{-}py)_2]^-$, 83665-26-3; $[(TPP)Cr(3,4\text{-}(CH_3)_2\text{-}py)_2]^-$, 83665-27-4; $EtCl_2$, 107-06-2; CH_2Cl_2, 75-09-2; PhCN, 100-47-0; PrCN, 109-74-0; $(CH_3)_2CO$, 67-64-1; THF, 109-99-9; DMF, 68-12-2; DMA, 127-19-5; Me_2SO, 67-68-5; py, 110-86-1.

Notes

Contribution from the Department of Energy and Environment, Brookhaven National Laboratory, Upton, New York 11973

Structural Consequences of Oxidation in Photosynthetic Models. Crystal Structure of (Perchlorato)-(5,10,15,20-tetraphenylporphinato)magnesium(II)

Kathleen M. Barkigia,* Len D. Spaulding, and Jack Fajer

Received April 7, 1982

The primary photochemical reactions in plant and bacterial photosynthesis consist of the transfer of an electron, in a picosecond time domain, from (bacterio)chlorophyll phototraps to nearby acceptors to yield (bacterio)chlorophyll π cation radicals.[1] Although structural investigations have provided detailed geometries for (bacterio)chlorophylls and their derivatives,[2-4] similar studies of the oxidized species have been precluded so far by the instability of the radicals, particularly their tendency to undergo oxidative dehydrogenations. As a model of the structural and stereochemical consequences of the loss of an electron in the photosynthetic chromophores, we present here an X-ray determination of a magnesium porphyrin radical, (perchlorato)(5,10,15,20-tetraphenylporphinato)magnesium(II) (**1**), $MgTPP^+ \cdot ClO_4^-$.[5]

The molecular structure of **1** and atom names are shown in Figure 1. (Experimental details are given in Table I, and fractional coordinates for the non-hydrogen atoms are presented in Table II.) Bond distances for the core of the macrocycle are displayed in Figure 2. The C_α–N, C_β–C_β, C_α–C_β, C_α–C_m, and C_m–C_{Ph} distances average 1.376 (3), 1.346 (4), 1.437 (3), 1.410 (3), and 1.493 (4) Å, respectively. They agree well with the corresponding bond lengths in $MgTPP(H_2O)$,[9] although the latter exhibits a fourfold symmetry. They are also consonant with those found in chlorophyllides (Chl) *a*[2] and *b*[3] and in the cation radical $ZnTPP^+ \cdot ClO_4^-$,[7] and with the

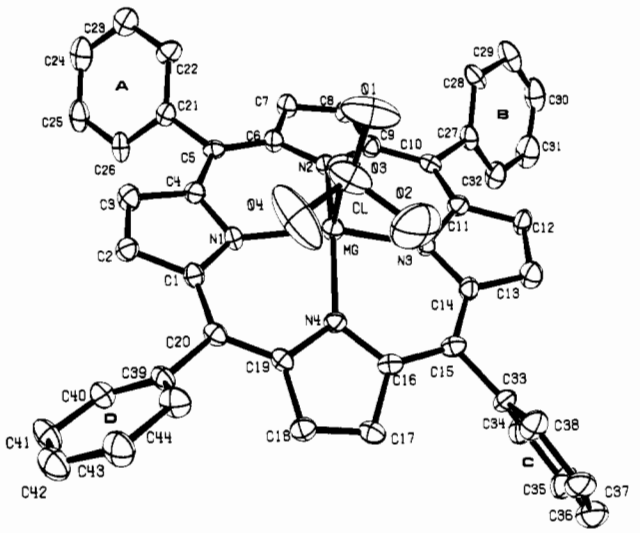

Figure 1. The structure of **1** and atom-numbering system. The thermal ellipsoids are drawn to enclose 50% probability. Hydrogen atoms have been omitted for clarity.

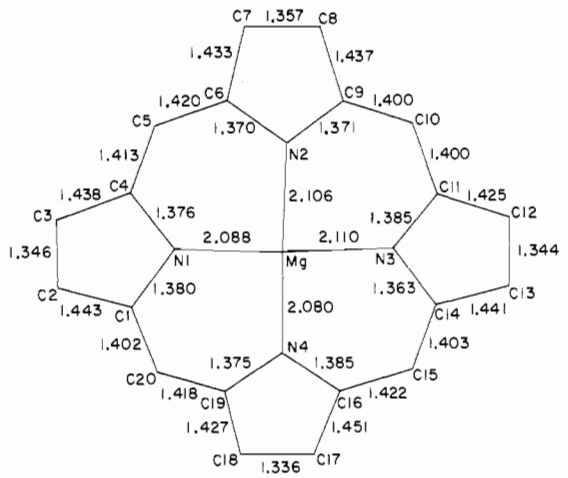

Figure 2. Bond distances (Å) for the core of **1**. The esd is 0.005 Å for a typical Mg–N bond and 0.008 Å for a C–C bond.

(1) (a) Fajer, J.; Fujita, I.; Davis, M. S.; Forman, A.; Hanson, L. K.; Smith, K. M. *Adv. Chem. Ser.* **1982**, *No. 201*, 489. (b) Davis, M. S.; Forman, A.; Hanson, L. K.; Thornber, J. P.; Fajer, J. *J. Phys. Chem.* **1979**, *83*, 3325 and references therein.
(2) (a) Chow, H. C.; Serlin, R.; Strouse, C. E. *J. Am. Chem. Soc.* **1975**, *97*, 7230. (b) Kratky, C.; Dunitz, J. D. *Acta Crystallogr., Sect. B* **1975**, *B31*, 1586.
(3) Serlin, R.; Chow, H. C.; Strouse, C. E. *J. Am. Chem. Soc.* **1975**, *97*, 7237.
(4) Barkigia, K. M.; Fajer, J.; Smith, K. M.; Williams, G. J. B. *J. Am. Chem. Soc.* **1981**, *103*, 5890.
(5) The radical was generated electrochemically at 0.6 V (vs. SCE) in dichloromethane containing 0.1 M tetrapropylammonium perchlorate as electrolyte[6] and isolated as described by Spaulding et al.[7] In solution, **1** exhibits optical and electron spin resonance spectra characteristic of $^2A_{2u}$ radicals.[6,8]
(6) Fajer, J.; Borg, D. C.; Forman, A.; Dolphin, D.; Felton, R. H. *J. Am. Chem. Soc.* **1970**, *92*, 3451.
(7) Spaulding, L. D.; Eller, P. G.; Bertrand, J. A.; Felton, R. H. *J. Am. Chem. Soc.* **1974**, *96*, 982.
(8) Fajer, J.; Borg, D. C.; Forman, A.; Felton, R. H.; Vegh, L.; Dolphin, D. *Ann. N.Y. Acad. Sci.* **1973**, *206*, 349.
(9) Timkovich, R.; Tulinsky, A. *J. Am. Chem. Soc.* **1969**, *91*, 4430.

0020-1669/83/1322-0349$01.50/0